RESEARCH ARTICLE



A new evolutionary preprocessing approach for classification of mental arithmetic based EEG signals

Ebru Ergün¹ · Onder Aydemir²

Received: 28 January 2020/Revised: 31 March 2020/Accepted: 11 April 2020/Published online: 23 April 2020 © Springer Nature B.V. 2020

Abstract

Brain computer interface systems decode brain activities from electroencephalogram (EEG) signals and translate the user's intentions into commands to control and/or communicate with augmentative or assistive devices without activating any muscle or peripheral nerve. In this paper, we aimed to improve the accuracy of these systems using improved EEG signal processing techniques through a novel evolutionary approach (fusion-based preprocessing method). This approach was inspired by chromosomal crossover, which is the transfer of genetic material between homologous chromosomes. In this study, the proposed fusion-based preprocessing method was applied to an open access dataset collected from 29 subjects. Then, features were extracted by the autoregressive model and classified by k-nearest neighbor classifier. We achieved classification accuracy (CA) ranging from 67.57 to 99.70% for the detection of binary mental arithmetic (MA) based EEG signals. In addition to obtaining an average CA of 88.71%, 93.10% of the subjects showed performance improvement using the fusion-based preprocessing method. Furthermore, we compared the proposed study with the common average reference (CAR) method and without applying any preprocessing method. The achieved results showed that the proposed method provided 3.91% and 2.75% better CA then the CAR and without applying any preprocessing method, respectively. The results also prove that the proposed evolutionary preprocessing approach has great potential to classify the EEG signals recorded during MA task.

Keywords Brain computer interface · Electroencephalography · Preprocessing · Evolutionary approach · Fusion method · Feature extraction · Classification

Introduction

The brain is the main control center of the human body. This control occurs when millions of nerve cells (neurons) that form the structural units of the central nervous system communicate with each other. The flow of information occurs throughout the brain and can be mapped via brain monitoring techniques such as electroencephalography (EEG), electrocorticography (ECoG),

☑ Ebru Ergün ebru.yavuz@erdogan.edu.tr

the magnetoencephalogram (MEG), functional magnetic resonance imaging (fMRI) (Aydemir and Kayikcioglu 2014; Forsyth et al. 2018). EEG is the most widely used monitoring technique through brain computer interfacing (BCI) researchers due to the advantages of high temporal resolution, non-invasiveness, cost-effectiveness and easy portability (Clarke et al. 2016) Researchers are able to recognize specific patterns of a person's brain signals relating to intent. A BCI system outputs these patterns into meaningful commands or messages to control outside devices or computers (Sharmila 2015; Ergün and Aydemir 2018a, b). Various signal processing algorithms are utilized to identify these patterns. Signal processing is an essential part of BCI systems because it helps to extract meaningful information from brain signals. The basic BCI module includes three main steps, which are the preprocessing, feature extraction and classification, concerned with the identification of different mental

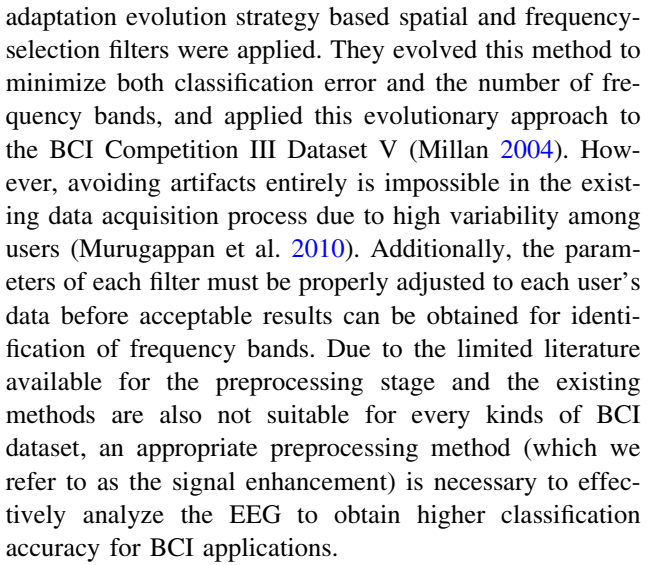


Department of Electrical-Electronics Engineering, Faculty of Engineering, Recep Tayyip Erdogan University, Rize, Turkey

Department of Electrical-Electronics Engineering, Faculty of Engineering, Karadeniz Technical University, Trabzon, Turkey

states (Lian et al. 2019). Among these, preprocessing is the step which requires special attention. Because the properly applied preprocessing step can increase the signal-to-noise ratio, remove unwanted artifacts in the data, reduce data dimensionality and emphasize portions of the data with discriminative power, it can affect the performance of a BCI system directly and significantly.

Various preprocessing methods are available in the literature, including methods for the removal of artifacts in EEG recordings (Wang et al. 2018; Kher and Gandhi 2016; Liu et al. 2019), the identification of relevant electrodes (Aydemir and Ergün 2019; Lahiri et al. 2017; Albasri et al. 2019), and the determination of effective frequency bands of EEG signals (Bashashati et al. 2007; Liu et al. 2014). Burger and Heever (2015) attempted to eliminate ocular artifacts (OA) to obtain a higher quality EEG for removing artifacts in EEG recordings. They proposed a new method combining independent component analysis and wavelet neural networking. They applied this method to the contaminated independent components, correcting the OA and thus lowering the amount of data lost. When they applied their methods to the dataset, they properly eliminated the OAs with very little data loss. Additionally, Somers et al. (2018) aimed to develop a generic EEG artifact removal algorithm which was based on the multi-channel Wiener filter, in which the artifact covariance matrix was replaced by a low-rank approximation based on the generalized eigenvalue decomposition. They applied the algorithm EEG dataset and removed EEG artifacts of various types. For the identification of relevant electrodes, Togha et al. (2019) proposed local activities estimation (LAE) based a preprocessing method to improve the performance of the motor imagery-based BCI system. They used the publicly available the BCI competition IV Dataset 1 (Blankertz et al. 2007) and the BCI competition III Dataset V (Millan 2004) datasets to evaluate the LAE and obtained 74.79% average classification accuracy (CA) for seven subjects. Rathee et al. (2017) evaluated the impact of EEG referencing schemes and spherical surface Laplacian methods on the classification performance of motor-imagery EEG datasets. They calculated the best CA to be 82.36% with current source density method for six binary classification tasks and two-class classification task by minimizing the effect of volume conduction in scalp level recordings. For the determination of effective frequency bands of EEG signals, Oh et al. (2014) introduced the Hjorth parameter (HP) and computed its Fisher ratio to determine the dominant frequency band and the timing in training EEG signals. After analyzing the EEG signals with the HP, they selected the principal frequency band and the timing using the Fisher ratio of the HP and obtained average of 79.1% CA for nine subjects. Another preprocessing method is proposed by Aler et al. (2012), where the covariance matrix



In this work, we have proposed a new preprocessing method for signal enhancement. We named it as fusionbased preprocessing method that enables the extraction of discriminative features because of enriches the signal. This method was inspired by chromosomal crossover, which refers to the transfer of genetic material between homologous chromosomes. Unlike other preprocessing methods, this study allows fusing the information in the two hemispheres of the brain, which provides to extract discriminative features. To do so, we applied this fusion-based preprocessing method to the EEG dataset recorded from 29 subjects. Then, the autoregressive (AR) model was used as a feature extracting method. We classified extracted features with k-nearest neighbor (k-NN) algorithm. In order to prove the success of the proposed method, we calculated CA, sensitivity (SE), specificity (SP) and kappa (κ) values. The results showed that the proposed method strongly improved the recognition of binary mental arithmetic based EEG signals.

The rest of this paper is organized as follows. Section two provides more information about the dataset and explains the methods, inducing the fusion-based preprocessing method, and feature extraction using AR model and k-NN classification algorithm. The experimental results, analysis and performance comparison are presented in section three, while the last section concludes the paper.

Materials and methods

Dataset description

EEG dataset was recorded from fourteen males and fifteen females [average age (years) 28.5 ± 3.7 (mean \pm standard deviation)] according to the declaration of Helsinki at the Technical University of Berlin (Shin et al. 2016). The



subjects were seated comfortably 1.6 m in front of a 50 inch white screen and told not to make any unnecessary movements apart from responding to the stimuli during the experiment. The experimental procedure is shown in Fig. 1 and included three sessions.

Each session was started with 60 s pre-rest period and ended up 60 s post-rest period. Following each pre-rest period, subjects were introduced to 2 s of a visual of a mental arithmetic (MA) task [an initial subtraction such as 'three-digit number minus one-digit number' 278–4)]. After the initial subtraction task in the center of the screen disappeared with a short beep, the subjects were asked to repeatedly subtract the one-digit number from the result of the previous subtraction while the EEG was recorded. For baseline tasks, no specific sign was introduced on the screen, and subjects were asked to take a rest without any thought during the 10 s task period. Next, each trial was ended with a 15–17 s resting period. Finally, the session was ended with a post-rest period. 20 trials were recorded in each session, for a total of 60 trials recorded in 3 sessions. Half of these trials were class a (MA task) and the rest were class b (baseline task). In this study, 50% of the trials were used for training and the rest were used for testing in the classification process. The EEG data was recorded using thirty electrodes (1. AFp1, 2. AFp2, 3. AFF1h, 4. AFF2h, 5. AFF5h, 6. AFF6h, 7. F3, 8. F4, 9. F7, 10. F8, 11. FCC3h, 12. FCC4h, 13. FCC5h, 14. FCC6h, 15. T7, 16 T8, 17. Cz, 18. CCP3h, 19. CCP4h, 20. CCP5h, 21. CCP6h, 22. Pz, 23. P3, 24. P4, 25. P7, 26. P8, 27. PPO1h, 28. PPO2h, 29. POO1, 30. POO2 and Fz for ground electrode) positioned according to the International 10-5 system. These electrodes are indicated with pink circles in Fig. 2. Moreover, the dataset was downsampled to 200 Hz and filtered with fourth order of Chebyshev type II filter (passband of 0.5–50 Hz).

Fusion based preprocessing method

In this study, we proposed a novel fusion method as preprocessing step, which provided more distinctive features. The fusion-based preprocessing method is a novel technique for evolutionary computation inspired by the process of chromosomal crossover. Chromosomal crossover refers

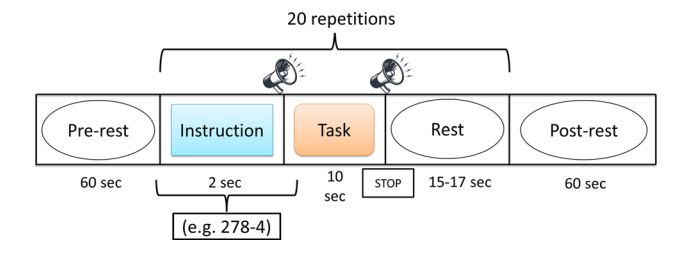


Fig. 1 Experimental procedure (Shin et al. 2016)

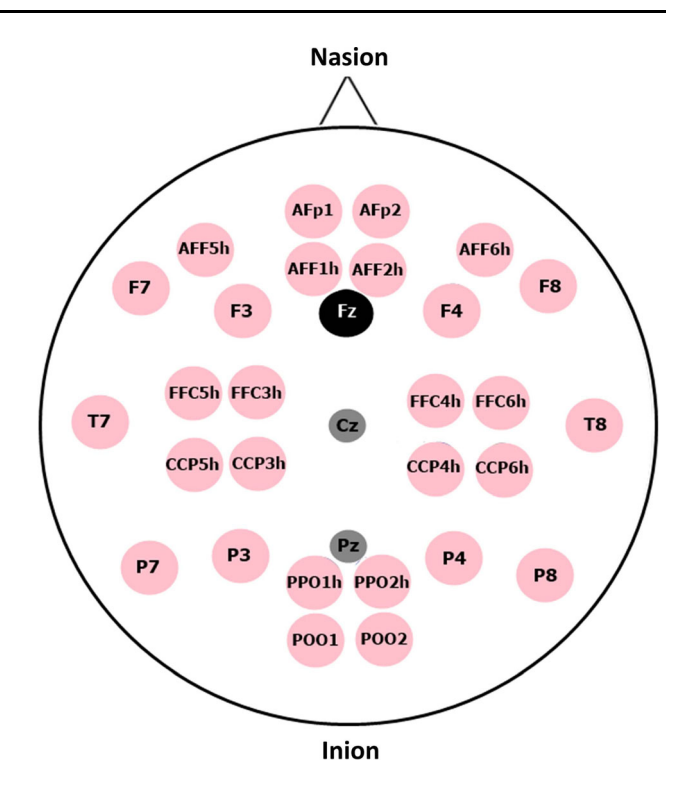


Fig. 2 Electrode positions (Shin et al. 2016)

to the transfer of genetic material (gene) that occurs between homologous chromosomes (Wu and Hickson 2003). Homologous chromosomes or pairs have the same length and chromosome central position, while each gene region carries the same characteristic genes. Within homologous chromosome pairs, one pair comes from the mother and the other from the father. During meiosis, synapsis occurs during the prophase-I stage and the homologous chromosomes are knotted together (Muller 1916). This node starts in the middle of the prophase-I phase and it takes to the end (Manhart and Alani 2016). During this time, peer regions of homologous chromosomes may be displaced. This is known as chromosomal crossover. Figure 3 illustrates this process step by step. In this fusion-based preprocessing method, homologous chromosome pairs may be likened to symmetrical channels, in which peer regions of homologous chromosomes are associated with the sample range. According to this point of view, the proposed method can be summarized as follows. The EEG signals were recorded from electrodes located at different places on the scalp of the user as shown in Fig. 2. In this figure, the inion and nasion points were considered border lines, dividing the skull into two hemispheres. Symmetrical channels on the left and the right of this line were identified as shown at Fig. 4a. The fusion of a single trial of symmetric channels a and a' is demonstrated in Fig. 4b, where n represents the sample transfer



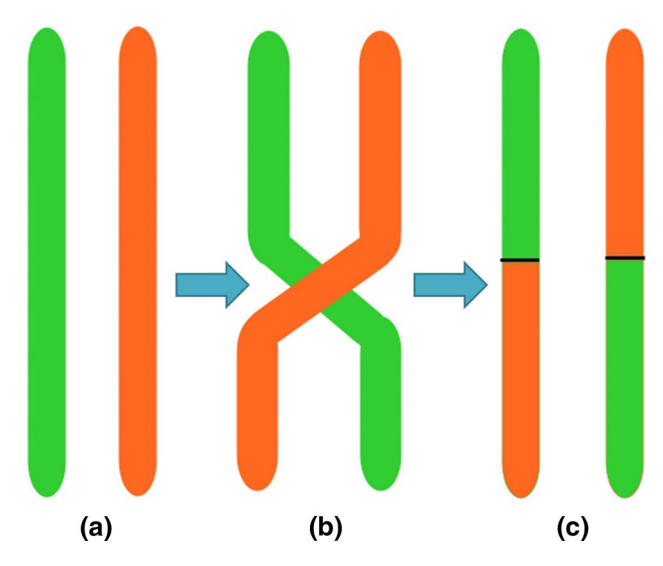


Fig. 3 Schematic representation of chromosomal crossover steps, **a** homologous chromosomes, **b** homologous chromosomes are knotted together, **c** Knotted homologous chromosomes

Furthermore, the fusions of a single trial of symmetrical channels a and a' with each other for n=2,3 and 4 are shown in Fig. 5, respectively. In this graph, while the x axis represents the time axis, the y axis represents the signal amplitude.

Feature extraction using an autoregressive model

The extraction of relevant information from an EEG signal is a feature which represents a distinguishing property or a recognizable measurement. An AR model is simply a linear regression of the current observation of the series against one or more prior observations of the series (Fenwick et al. 1969; Zhang et al. 2018; Sun et al. 2019). The AR model of order *b* for a single channel can be written as:

$$x(t) = \sum_{i=1}^{b} \beta_i x(t-i) + \epsilon_t \tag{1}$$

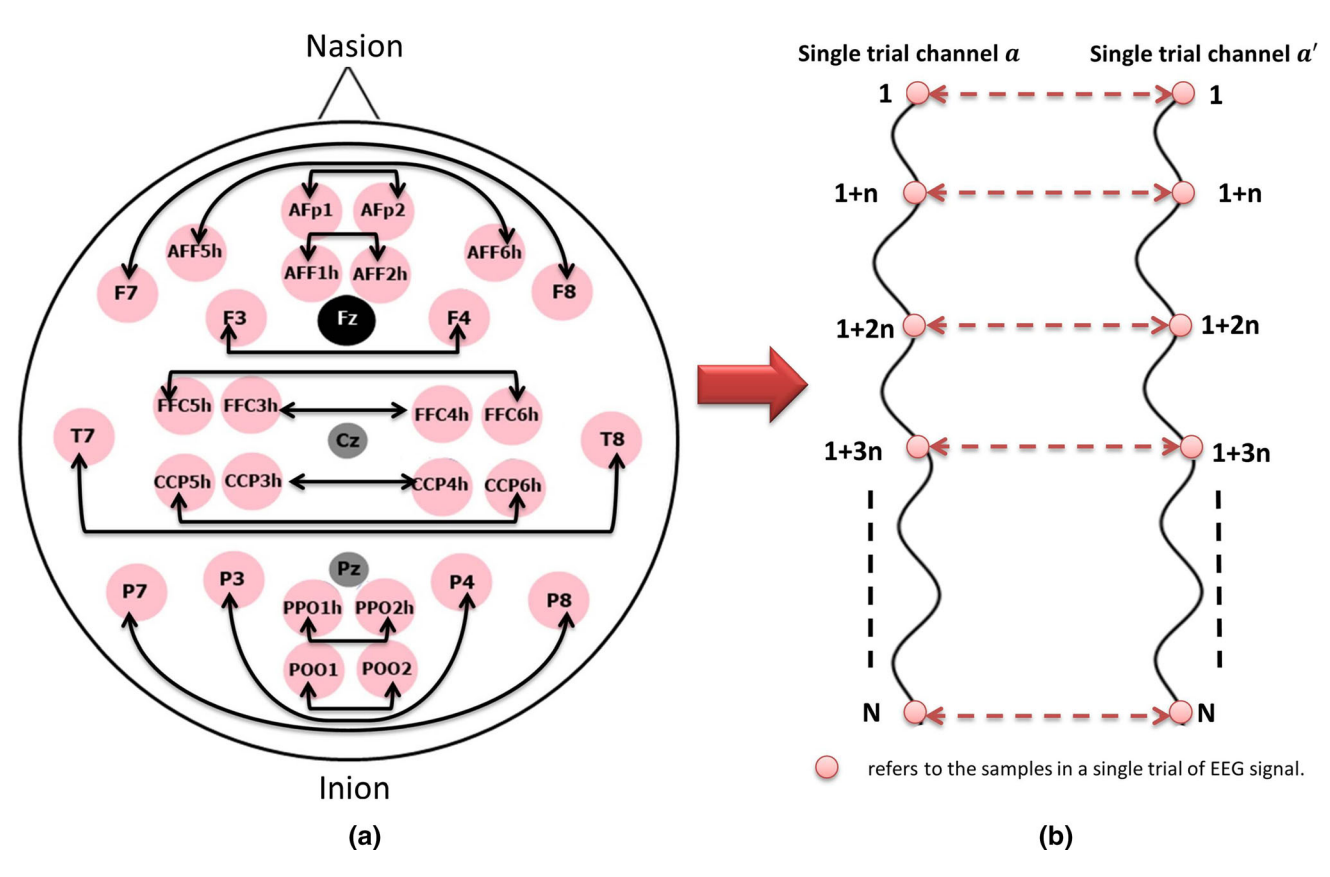


Fig. 4 Fusion-based preprocessing method **a** symmetrical channels according to inion and nasion point where the representation of symmetrical channels with each other is indicated by black arrows. **b** Data fusion for single EEG trial of each channel

rate, which means the samples are replaced (fused) in n interval through the symmetrical channels.

Exemplary signal (artificial signal) representation for symmetric channels a and a' was also plotted in Fig. 5.

where x(t) (raw EEG signal), β_i (i = 1, 2, ..., b) and ϵ_t are the column vector of time series data, the *b*-order AR model coefficients and white noise (independent from the previous points), respectively. Additionally, b presents the



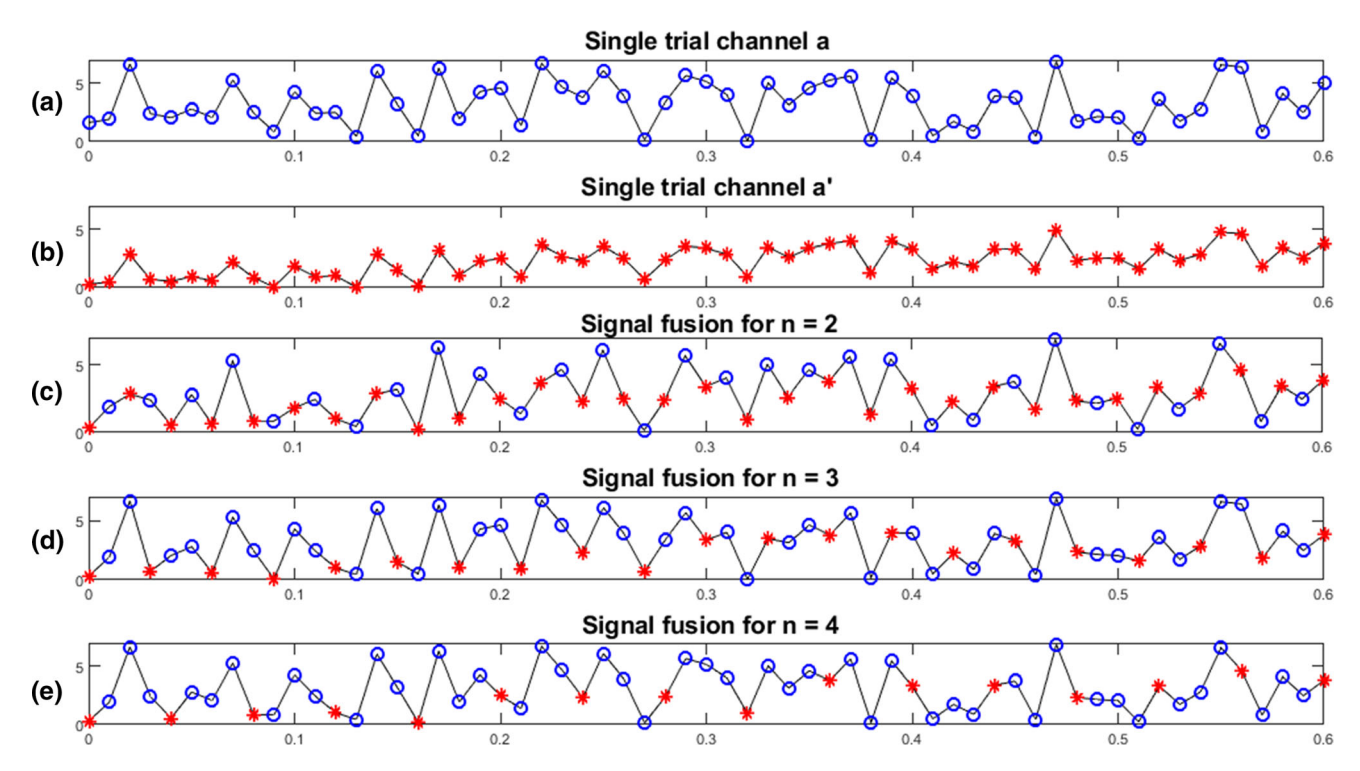


Fig. 5 Signal representation for artificially generated signal (the x axis represents the time axis and the y axis represents the signal amplitude), **a** Single trial of channel a, where circle points indicate the samples), **b** symmetry of channel a(a'), where star points indicate

samples, **c** fused version of a and a' for n = 2, **d** fused version of a and a' for n = 3, e) Fused version of a and a' for n = 4

order of the AR model, which indicates that current observation depends on b past observations. For an example, if order of an AR model is four then β_1 , β_2 , β_3 , and β_4 are calculated according to Eq. (1). It is worthwhile mentioning that the order of AR model is a vital parameter to obtain discriminative features. In this study, we searched the best order for each subject between 1 and 12 using the cross-validation method on the training set.

Classification Using k-Nearest Neighbor

The *k*-nearest neighbor method is a well-known supervised classification technique introduced by Fix and Hodges (1951). It has been widely used in the machine learning community because it is easy to implement, analytically traceable and resistant to noisy training sets (Ergün and Aydemir 2018a, b; Sabancı and Koklu 2015). This algorithm stores all available data points and classifies new data points based on a similarity measure. For a classification task, the *k*-NN algorithm consists of two phases, namely the training phase and classification phase. While the training phase contains multi-dimensional feature vectors with class labels, unclassified test trials in a training dataset are categorized based on their distance to points in the classification phase. Also, each test trial is assigned to the class to which most of the *k* nearest neighbors belong.

There are many distance measurement techniques, including Euclidean, cityblock, cosine, Manhattan and Minkowski. We used the city block distance metric, which represents the distance between points in a city road grid. Given a $[ma \times c]$ data matrix a, which is treated as $[ma(1 \times c)]$ row vectors $a_1, a_2, a_3, \ldots a_{ma}$ and $[mb \times c]$ data matrix b, which is treated as $[mb(1 \times c)]$ row vectors $b_1, b_2, b_3, \ldots b_{mb}$ distances between the vector a_r and b_p is the sum of the absolute differences of their coordinates as defined using the following equation:

$$d_{rp} = \sum_{i=1}^{c} \left| a_{ri} - b_{pi} \right| \tag{2}$$

where c represents the number of features.

Moreover, it is important to note that we applied the proposed classification procedure 100 times to avoid the problems of random selections in training and test sets. Then, we calculated the average CA, SE, SP and κ (Kumar et al. 2017) metric values to evaluate the performance of the classifier. These metrics were obtained from the confusion matrix parameters as shown in Table 1. In this table, the MA and the baseline task trials were signified as A and B, respectively. Based on these table parameters, we calculated the respective CA, SE, SP and κ values as follows:



Table 1 Confusion matrix

Confusion matrix		Predicted class		Total
		A	В	
Actual class	A	True A	False B	H_{11} = True A + False B
	B	False A	True B	H_{21} = False A + True B
Total		H_{12} = True A + False A	H_{22} = False B + True B	$H = H_{11} + H_{21}$

$$CA = \frac{(\text{True } A + \text{True } B)}{H} \times 100 \tag{3}$$

$$SE = \frac{(\text{True } A)}{H_{12}} \times 100 \tag{4}$$

$$SP = \frac{(\text{True } B)}{H_{22}} \times 100 \tag{5}$$

$$\kappa = \frac{\alpha_0 - \alpha_e}{1 - \alpha_e} \tag{6}$$

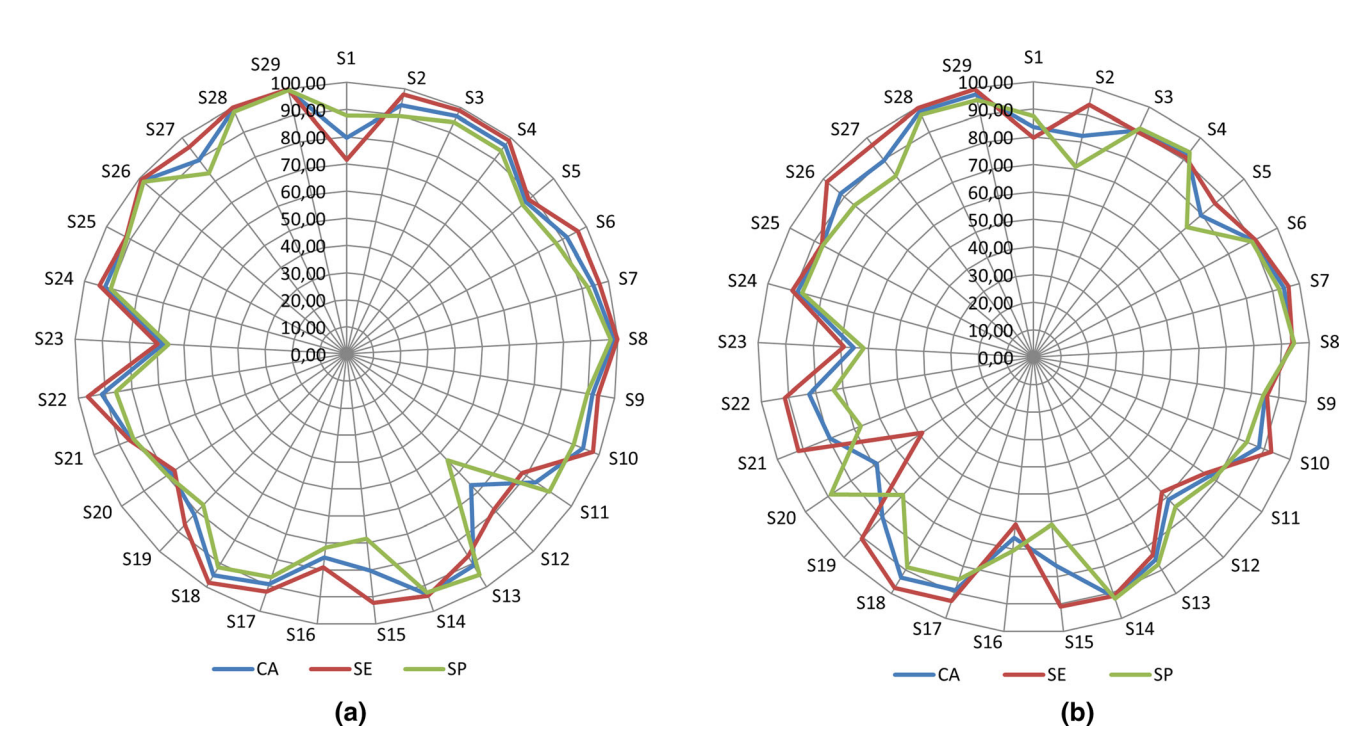
where

$$\propto_0 = \frac{\text{True } A + \text{True } B}{H} \tag{7}$$

$$\propto_e = \frac{[H_{11} \times H_{12}] + [H_{21} \times H_{22}]}{H^2}$$

Results

The classification results with fusion and without applying any preprocessing methods are given in Fig. 6 with a radar plot. As seen from this figure, while the highest CA was achieved as 99.13% for Subject 29, the lowest CA was calculated as 66.50% for Subject 12 with the fusion-based preprocessing method. Additionally, in this stage the minimum and maximum SE and SP values were obtained between 69.53-99.93% and 54.00-99.53%, respectively. On the other hand, the highest CA was achieved as 98.30% for Subject 28, whereas the lowest CA was calculated as 65.33% for Subject 23 without using any preprocessing method. Furthermore, at this stage, the minimum and maximum SE and SP values were calculated between 48.80-99.60% and 61.07-97.00%, respectively. For the detail performance evaluation, we also obtained the κ



(8)

Fig. 6 CA, SE and SP values a with fusion-based preprocessing method b without applying any preprocessing method



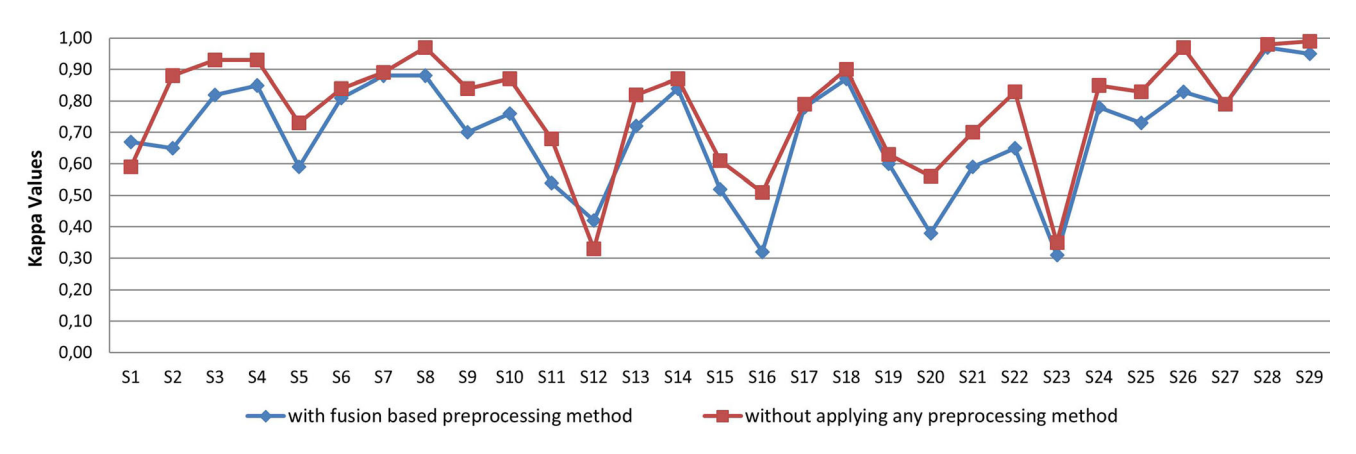


Fig. 7 Kappa values

values as shown in Fig. 7. The κ values were calculated between 0.35 and 0.99 with the fusion-based preprocessing method. We got the average CA, SE, SP and κ values with this method as 88.71%, 90.85%, 86.57% and 0.77, respectively.

As seen in Fig. 8, the fusion-based preprocessing method showed significant CA improvement for most of the subjects against without applying any preprocessing. While the best percentage improvement was for Subject 2 as 4.06%, the worst positive increment was for Subject 27 as 0.06% In contrast, Subject 1 and Subject 12 showed performance decreasing. Eventually, it should be emphasized that 27 of 29 subjects showed performance improvement with the proposed fusion-based preprocessing method. Additionally, the proposed method increased the total performance 3.91% when calculating the average of 29 subjects.

In this study, sample transfer rate is an important parameter that influences performance because samples are fused in n ranges. This parameter was specifically determined for each subject by cross validation procedure in the

range of 1–10. The values given in is shown in Fig. 9. Also, the orders of the AR model (b) for each subject are shown in Fig. 10. In all these graphs, the subjects from 1 to 29 are expressed as S1, S2, S3.....S29, respectively.

In this research, the proposed approach was compared to the CAR method, which is commonly used in EEG based BCI applications (Gliske et al. 2016). The effectiveness of this method was tested in terms of CA and the results are given in Table 2, showing that the average CA using the fusion-based preprocessing method was 2.75% higher than the CAR method. Additionally, it can be seen from this table that our method also outperformed the result of Shin et al. (2016) and the result of without applying preprocessing procedure. The obtained results also showed that the AR model features can be effectively used to represent MA based EEG signals in order to prove the validity of the proposed method over without preprocessing procedure, the Wilcoxon Signed Rank test was evaluated. There were statistically significant differences (p < 0.001) found in terms of classification accuracy improvement. Based on these results it can be mentioned that the fusion-based

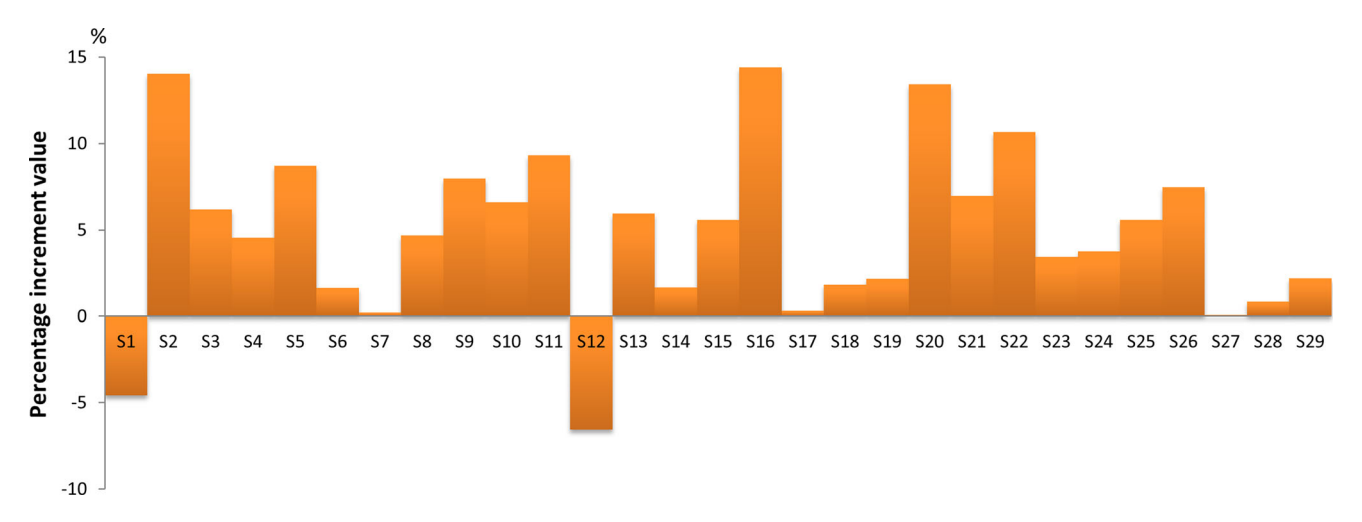


Fig. 8 Percentage increment value for each person by the fusion-based preprocessing method



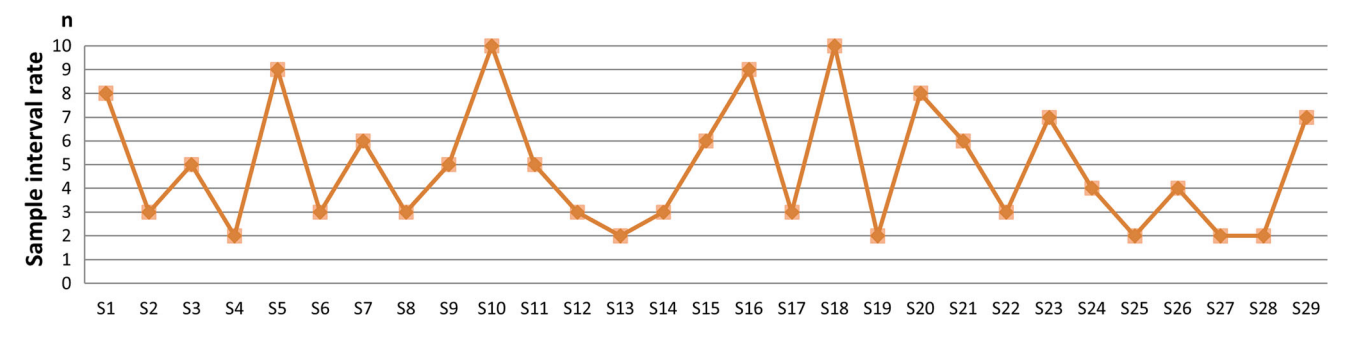


Fig. 9 Sample interval rate for each person by the fusion-based preprocessing method

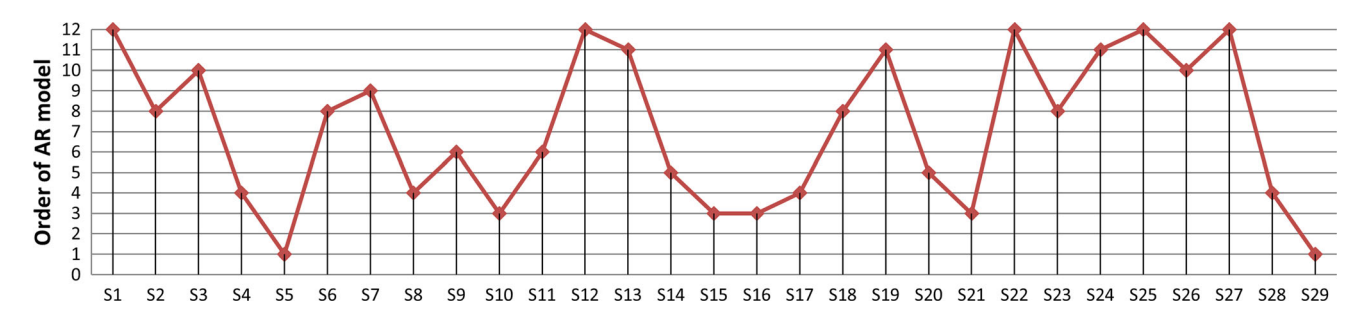


Fig. 10 Order of the AR model for each Subject

Table 2 Performance comparison

Methods	CA (%)	
CAR	85.96	
Without preprocessing	84.80	
Fusion (proposed) method	88.71	
Shin et al. (2016)	75.90	

preprocessing method has great potential to improve BCI system performance.

Conclusion

In this paper, a novel fusion preprocessing method has been successfully applied to EEG dataset recorded from 29 subjects. The proposed method allows extraction of discriminative AR features by fusing the information in the two hemispheres of the brain and it has great potential to improve the CA performance of MA based EEG signals. It is noteworthy that we calculated the average CA, SE, SP and κ values as 88.71%, 90.85%, 86.57% and 0.77, respectively. It must also be emphasized that 93.10% of the subjects showed performance improvement with the fusion-based preprocessing method. More specifically, in order to show its capacity, we compared the method with mostly used preprocessing method of CAR, where our

method provided an improvement of 2.75% over it. Consequently, we believe that the proposed method can be successfully applied MA based EEG signals for enhancing the BCI system performance.

As future work, we intend to improve CA performance in two ways. One of them is applying the proposed method to a hybrid BCI dataset, which includes EEG functional near-infrared spectroscopy signals. Secondly, we aim to extend our approach by utilizing channel selection methods including binary gravitation search and particle swarm optimization algorithms in order to improve CA performance with small number of channels.

Acknowledgements Ebru Ergun's contribution was supported by a scholarship from The Scientific and Technological Research Council of Turkey (TUBITAK).

References

Albasri A, Abdali-Mohammadi F, Fathi A (2019) EEG electrode selection for person identification thru a genetic-algorithm method. J Med Syst 43(9):297

Aler R, GalváN IM, Valls JM (2012) Applying evolution strategies to preprocessing EEG signals for brain–computer interfaces. Inf Sci 215:53–66

Aydemir O, Ergün E (2019) A robust and subject-specific sequential forward search method for effective channel selection in brain computer interfaces. J Neurosci Methods 313:60–67

Aydemir O, Kayikcioglu T (2014) Decision tree structure based classification of EEG signals recorded during two dimensional cursor movement imagery. J Neurosci Methods 229:68–75



- Bashashati A, Fatourechi M, Ward RK, Birch GE (2007) A survey of signal processing algorithms in brain-computer interfaces based on electrical brain signals. J Neural Eng 4(2):R32
- Blankertz B, Dornhege G, Krauledat M, Müller KR, Curio G (2007) The non-invasive Berlin brain–computer interface: fast acquisition of effective performance in untrained subjects. NeuroImage 37(2):539–550
- Burger C, van den Heever DJ (2015) Removal of EOG artefacts by combining wavelet neural network and independent component analysis. Biomed Signal Process Control 15:67–79
- Clarke AR, Barry RJ, Indraratna A, Dupuy FE, McCarthy R, Selikowitz M (2016) EEG activity in children with Asperger's syndrome. Clin Neurophysiol 127(1):442–451
- Ergün E, Aydemir Ö (2018a) Decoding of binary mental arithmetic based near-infrared spectroscopy signals. In: 2018 3rd international conference on computer science and engineering (UBMK). IEEE, pp 201–204
- Ergün E, Aydemir Ö (2018b) Classification of motor imaginary based Near-Infrared spectroscopy signals. In: 2018 26th signal processing and communications applications conference (SIU). IEEE, pp 1–4
- Fenwick PB, Mitchie P, Dollimore J, Fenton GW (1969) Application of the autoregressive model to EEG analysis. Agressologie: revue internationale de physio-biologie et de pharmacologie appliquees aux effets de l'agression 10:Suppl-553
- Fix E, Hodges JL Jr (1951) Discriminatory analysis-nonparametric discrimination: consistency properties. California Univ Berkeley
- Forsyth A, McMillan R, Campbell D, Malpas G, Maxwell E, Sleigh J, Muthukumaraswamy SD (2018) Comparison of local spectral modulation, and temporal correlation, of simultaneously recorded EEG/fMRI signals during ketamine and midazolam sedation. Psychopharmacology 235(12):3479–3493
- Gliske SV, Irwin ZT, Davis KA, Sahaya K, Chestek C, Stacey WC (2016) Universal automated high frequency oscillation detector for real-time, long term EEG. Clin Neurophysiol 127(2):1057–1066
- Kher R, Gandhi R (2016) Adaptive filtering based artifact removal from electroencephalogram (EEG) signals. In: 2016 international conference on communication and signal processing (ICCSP). IEEE, pp 561–564
- Kumar S, Sharma A, Tsunoda T (2017) An improved discriminative filter bank selection approach for motor imagery EEG signal classification using mutual information. BMC Bioinform 18(16):545
- Lahiri R, Rakshit P, Konar A (2017) Evolutionary perspective for optimal selection of EEG electrodes and features. Biomed Signal Process Control 36:113–137
- Lian J, Bi L, Fei W (2019) A novel event-related potential-based brain-computer interface for continuously controlling dynamic systems. IEEE Access 7:38721–38729
- Liu Q, Chen K, Ai Q, Xie SQ (2014) Recent development of signal processing algorithms for SSVEP-based brain computer interfaces. J Med Biol Eng 34(4):299–309

- Liu J, Sheng Y, Zeng J, Liu H (2019) Corticomuscular coherence for upper arm flexor and extensor muscles during isometric exercise and cyclically isokinetic movement. Front Neurosci 13:522
- Manhart CM, Alani E (2016) Roles for mismatch repair family proteins in promoting meiotic crossing over. DNA Repair 38:84–93
- Millan JR (2004) On the need for on-line learning in brain-computer interfaces. IEEE Int Joint Conf Neural Netw 4:2877–2882
- Muller HJ (1916) The mechanism of crossing-over. Am Nat 50(592):193-221
- Murugappan M, Ramachandran N, Sazali Y (2010) Classification of human emotion from EEG using discrete wavelet transform. J Biomed Sci Eng 3(4):390
- Oh SH, Lee YR, Kim HN (2014) A novel EEG feature extraction method using Hjorth parameter. Int J Electron Electr Eng 2(2):106–110
- Rathee D, Raza H, Prasad G, Cecotti H (2017) Current source density estimation enhances the performance of motor-imagery-related brain-computer interface. IEEE Trans Neural Syst Rehabil Eng 25(12):2461-2471
- Sabancı K, Koklu M (2015) The classification of eye state by using kNN and MLP classification models according to the EEG signals. Int J Intell Syst Appl Eng 3(4):127–130
- Shin J, von Lühmann A, Blankertz B, Kim DW, Jeong J, Hwang HJ, Müller KR (2016) Open access dataset for EEG+ NIRS single-trial classification. IEEE Trans Neural Syst Rehabil Eng 25(10):1735–1745
- Sharmila A (2015) Signal processing algorithm for brain computer interface—a review. World Appl Sci J 33(5):715–721
- Sun L, Jin B, Yang H, Tong J, Liu C, Xiong H (2019) Unsupervised EEG feature extraction based on echo state network. Inf Sci 475:1–17
- Somers B, Francart T, Bertrand A (2018) A generic EEG artifact removal algorithm based on the multi-channel Wiener filter. J Neural Eng 15(3):036007
- Togha MM, Salehi MR, Abiri E (2019) Improving the performance of the motor imagery-based brain-computer interfaces using local activities estimation. Biomed Signal Process Control 50:52-61
- Wang K, Li W, Dong L, Zou L, Wang C (2018) Clusteringconstrained ICA for ballistocardiogram artifacts removal in simultaneous EEG-fMRI. Front Neurosci 12:59
- Wu L, Hickson ID (2003) The Bloom's syndrome helicase suppresses crossing over during homologous recombination. Nature 426(6968):870
- Zhang Y, Zhang S, Ji X (2018) EEG-based classification of emotions using empirical mode decomposition and autoregressive model. Multimed Tools Appl 77(20):26697–26710

Publisher's Note Springer Nature remains neutral with regard to jurisdictional claims in published maps and institutional affiliations.

